ISSN 1061-8309, Russian Journal of Nondestructive Testing, 2020, Vol. 56, No. 5, pp. 435–444. © Pleiades Publishing, Ltd., 2020.

RADIO WAVE METHODS

Model Test Study on Oil Leakage and Underground Pipelines Using Ground Penetrating Radar

Lei Gao[a, b, c, *], Hantao Song[a], Hanlong Liu[d], Chuan Han[a], and Yumin Chen[a]

[a]*Key Laboratory of Ministry of Education for Geomechanics and Embankment Engineering, Hohai University, Nanjing, Jiangsu, 210098 China*

[b]*Key Laboratory of Hydraulic and Waterway Engineering of the Ministry of Education, Chongqing Jiaotong University, Chongqing, 400074 China*

[c]*National Engineering Research Center for Inland Waterway Regulation, Chongqing Jiaotong University, Chongqing, 400074 China*

[d]*School of Civil Engineering, Chongqing University, Chongqing, 400045 China*

**e-mail: gaoleihhu@hhu.edu.cn*

Received August 9, 2018; revised August 9, 2018; accepted December 27, 2019

Abstract—The underground pipelines have frequent ruptures and leakage problems in the urban area, the distribution of contaminated soil is difficult to monitor and evaluate. It is important that the effective identification and assessment of underground pipelines and contaminated soil. The ground penetrating radar was applied to the detection of underground pipelines and contaminated soil using the electromagnetic wave propagation. The detection tests were carried out on pipes and leaking oil with different sizes, materials and buried depths in a transparent model tank developed by ourselves. The radar signal is processed by using GRED HD software, the single-channel waveform of underground pipelines and contaminated soil are obtained. The time-domain finite difference method is used to analyze the non-stationary signals of ground penetrating radar. The radar signals of underground pipelines with different characteristics and the variation of leakage oil are discussed. The radar interpretation accuracy of underground pipelines and contaminated soil is improved. It will provide the reference for related studies in future.

Keyword: underground pipelines, contaminated soil, ground penetrating radar, model test, finite difference in time domain

DOI: 10.1134/S1061830920050058

1. INTRODUCTION

The distribution of underground pipelines as urban lifelines is becoming more and more complex in the rapid urbanization [1–5]. Most cities have not yet established a complete underground pipeline network and management system[6–12]. With the incomplete or missing relevant data, the engineering accidents caused by excavation of underground pipelines have occurred in many areas of all over world, the problems of pipeline leakage are particularly acute [13–15]. The usual detection method is to excavate the pipelines randomly and the operation is cumbersome. It is difficult to find the hidden diseases of pipeline [16–19]. The ground penetrating radar technology has the characteristics of high efficiency, non-destructiveness, high precision, good detection effect on underground buried objects [20–23]. It can well meet the detection requirements of underground pipelines and contaminated soil [24–27]. However, the typical ground penetrating radar image of underground pipelines and their spectral characteristics are lacking. It cannot judge the underground pipelines without providing accurate information on the location, the material of the pipeline and the contaminated soil generated by the pipeline leakage oil. There is also a lack of relevant research on the variation of migration distribution. This paper attempts to carry out the study on the underground pipeline and leaking oil using ground penetrating radar technology, the data are analyzed, the signal characteristics of underground pipeline and contaminated soil are obtained.

(a) Radar host (b) 1600 MHz antenna (c) 400 MHz antenna (d) 100 MHz antenna

Fig. 1. Host and antenna of ground penetrating radar.

Fig. 2. Model tank.

2. TEST OF OIL LEAKAGE AND UNDERGROUND PIPELINES

2.1. Test Equipment and Devices

This test equipment uses Italian RIS series high-frequency ground penetrating radar IDS (shown in Fig. 1). It is portable with high transmission rate, fast scanning speed, good antenna shielding, frequency bandwidth, strong signal stability, high resolution, high sensitivity, waterproof, dustproof, etc. The frequency of complete antenna is from 25 to 2500 MHz including ground-coupled antenna, air-coupled antenna, and various antenna arrays. It can meet most extensive detection needs.

In order to facilitate the material placement and observation during the model test, the economic factors are considered, the model tank with transparent fiber reinforced plastic material is made to contain the soil (see Fig. 2). The internal dimensions of the model tank are 80 cm × 40 cm × 50 cm (length × width × high). After several pre-detection tests, it is confirmed that the model tank has little influence on the ground penetrating radar detection.

The test selected the air drying sand with uniform soil (as shown in Fig. 3) as the backfill to minimize the influence of soil layer on the detection results. The air drying sand has a particle size of 0.25–0.5 mm and the filling density is 1900 kg/m^3. The filling height is 0.4 m and the distance is 10 cm away, which is convenient for the radar detection. The separate pipes of different materials are prepared. It can be seen in Table 1 for details.

The lubricating oil is used as the pipeline filling medium during the test. In order to simulate the process of oil leakage in the pipeline, the oil is injected into the pipeline through the water pipe connected to the pipeline.

Table 1. Parameters of pipelines

Material	Diameter	Length, cm
Polyvinylchloride pipe (PVC)	DN63 (63 mm)	70
Polyethylene pipe (PE)		70
Cast iron pipe		70

Fig. 3. Air drying sand.

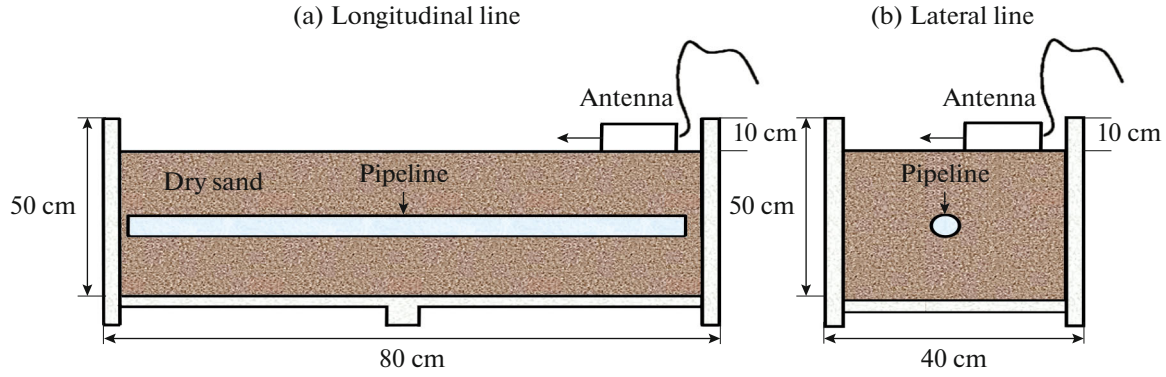

Fig. 4. Different line directions.

2.2. Direction of Antenna

In the test, the direction of pipe is parallel to the long axis of the model tank. The line arrangement is selected to arrange in three directions parallel to the pipe (longitudinal line) and perpendicular to the pipe (lateral line). The antenna is used to swipe the surface of sand to detect the pipe. The specific operation is shown in Fig. 4.

2.3. Test Procedures

The procedure is divided into four working conditions, which are the difference of radar characteristic signals of pipelines with different pitches, different depths, different materials, and the variation of oil pollution leaks from pipelines. The diagram of test procedure is shown in Fig. 5.

(1) The sand is filled with the height of 20 cm in the model tank, three PVC pipes in parallel at intervals of 5 cm are placed, then the sand is filled with the height of 40 cm. The ground penetrating radar is used to detect and collect information according to the predetermined line. The above procedure was repeated, the interval between the three pipes was set to 6, 7, 8, 9, and 10 cm respectively. The total of 5 parallel tests was performed.

(2) The PVC pipe is put into the model tank when it is filled with the height of 10 cm, then then the sand is filled with the height of 40 cm. The ground penetrating radar is used to detect and collect information according to the predetermined line. The above procedure was repeated, the PVC pipe is put into the model tank when it is filled with the height of 20, 30 cm. The total of 3 parallel tests was performed.

(3) The PVC pipe is put into the model tank when it is filled with the height of 20 cm, then the sand is filled with the height of 40 cm. The ground penetrating radar is used to detect and collect information according to the predetermined line. The above procedure was repeated, the PE and cast iron pipe are put into the model tank separately when it is filled with the height of 20 cm. The total of 3 parallel tests was performed.

(4) The sand is filled with the height of 20 cm in the model tank, the PVC pipe is drilled a hole in the center. The plastic hoses are connected at both ends of the PVC pipe and the pipe is put into the model

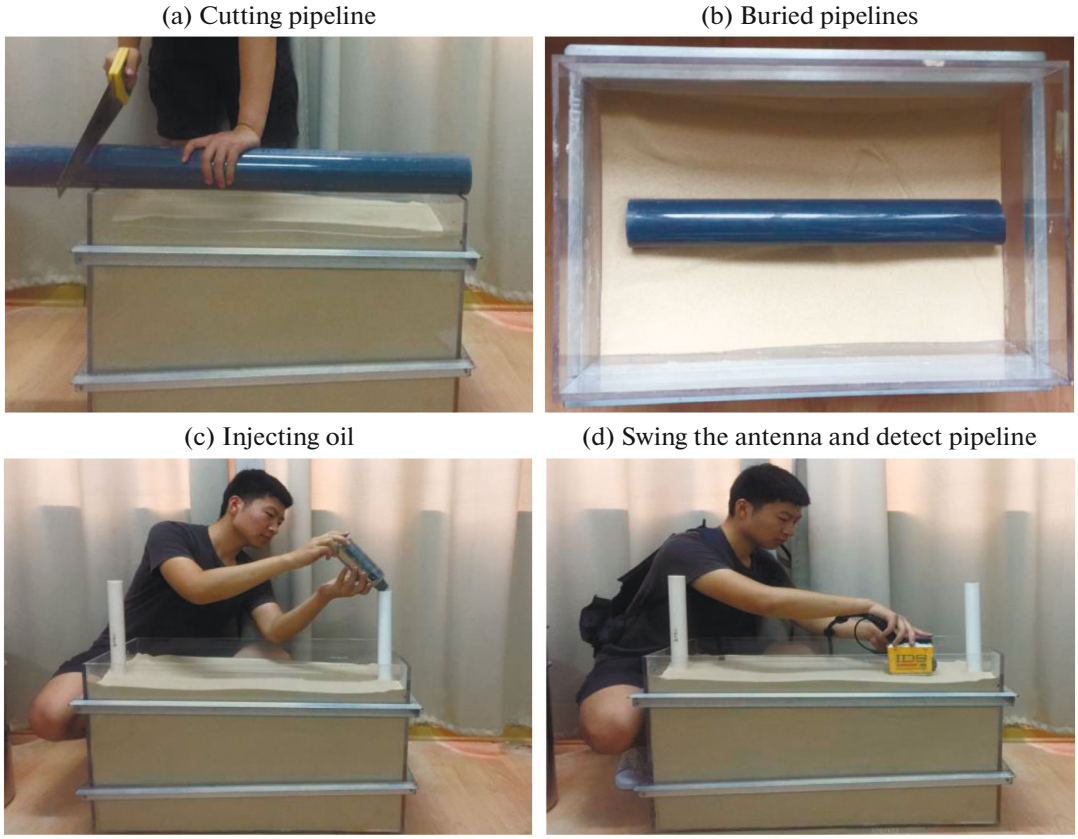

Fig. 5. Diagram of test procedure.

tank. Then the sand is filled with the height of 40 cm, the hose are connected outside the tank, the lubricating oil is injected into the PVC pipe from the plastic hose to simulate the oil leakage process. The ground penetrating radar is used to detect and collect information according to the predetermined line. The above procedure was repeated to investigate the variation of radar signals for oil around the pipeline.

(5) After the information is obtained, the original image is processed and analyzed using the signal processing software GRED HD.

All of the pipe axes are parallel to the long side of model tank, and the pipe axis is always horizontally located in the center of the wide side of the model tank. The process of the model test is shown in Fig. 6.

3. RESULTS

3.1. Test Phenomenon

Taking the second horizontal line data of PVC pipe with a depth of 10 cm in working condition 2 as an example, the operation flow and processing effect of ground penetrating radar signal preprocessing using GRED HD are shown. This test uses the ground penetrating radar with an antenna frequency of 1600 MHz, a sampling window of 12 ns, and a sampling point of 512. The original radar image is shown in Fig. 7.

There is a strong direct wave around 1.2 ns. The direct wave is a strong reflection signal caused by the electromagnetic wave propagating in the air. It consists of two parts: the electromagnetic wave directly transmits by the transmitting antenna to the receiving antenna and the electromagnetic wave reflects by the surface of medium. The waveform data below the direct wave is poorly defined. When the time is 3.0 ns, there is almost no waveform data visible, and the medium interface between the soil and pipeline cannot be distinguished. Therefore, it is necessary to process the data of radar signal, including direct wave removal, background removal, band pass filtering, signal gain and the like, it can perform deeper interpretation of the radar image to identify and evaluate the underground pipeline.

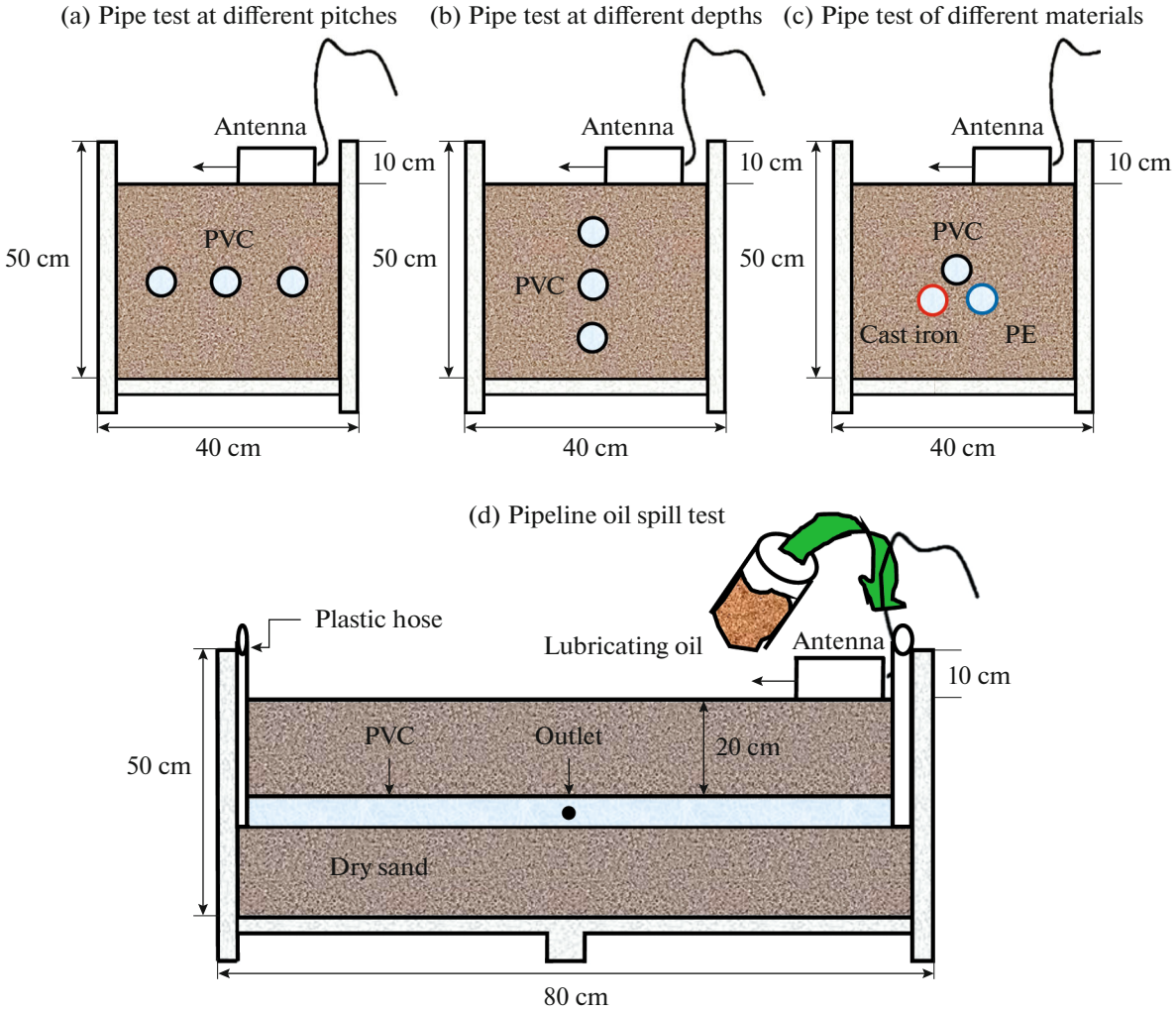

Fig. 6. Process of the model test.

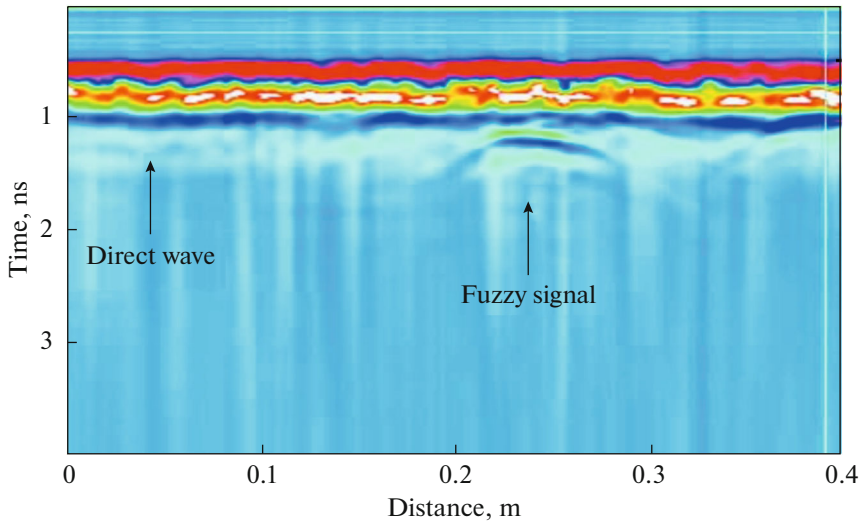

Fig. 7. Ground penetrating radar original image at line 5.

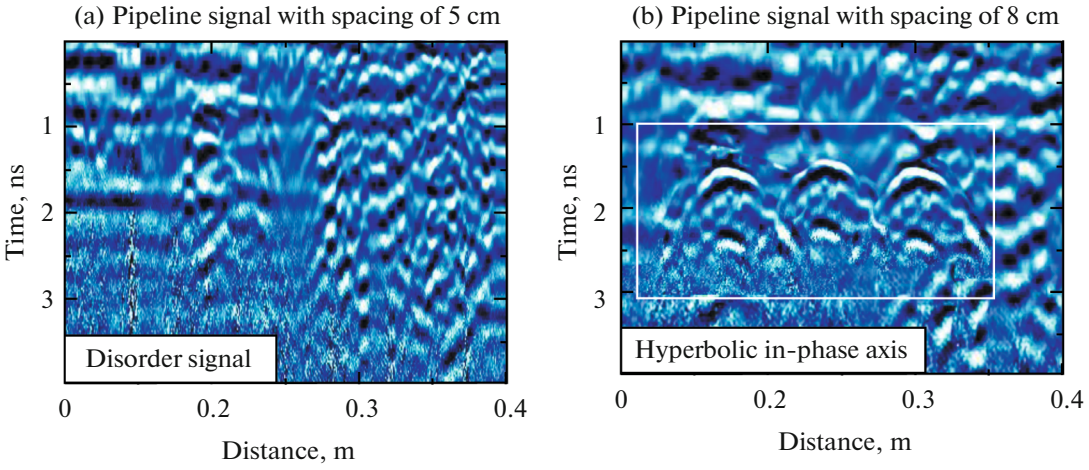

Fig. 8. Radar signal image of different spacing pipelines.

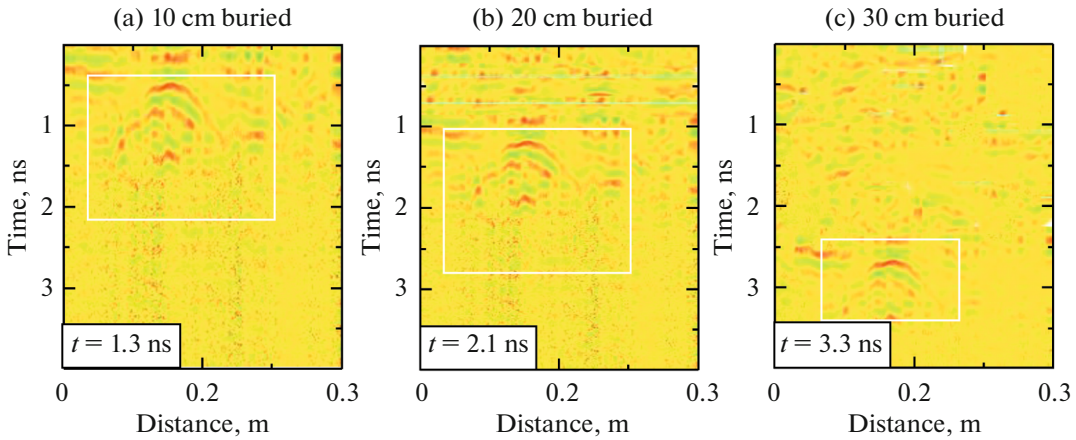

Fig. 9. Radar signal image of different spacing of pipelines.

3.2. Signal Analysis of Pipeline with Different Distance

The radar signal profile of different pitch pipes is shown in Fig. 8. The hyperbolic characteristics of pipeline are basically not distinguished in Fig. 8a. Because the pipe spacing is too small, the reflected electrical waves interfere with each other seriously, resulting in failure to properly image and the signal is more turbulent. The typical hyperbolic in-phase axis signal of the underground pipeline can be seen in Fig. 8b with a distance of 7 cm. According to the corresponding distance of the three hyperbolic inflection points on the radar profile, the pipeline spacing can be roughly inferred almost about 8 cm, the three pipelines can be clearly distinguished.

The test shows that the ground penetrating radar can detect small-caliber pipes. The horizontal resolution of pipeline for the 1600 MHz antenna detection should be about 8 cm.

3.3. Signal Analysis of Pipeline with Different Depth

A cross-sectional view of the radar signal for different depth pipes is shown in Fig. 9. The electromagnetic waves are reflected at the interface of medium, and the vibrations are generated on the single-channel waveform. The amplitude of direct wave is large, and the amplitude is greatly attenuated after entering the underground. The time coordinate value at the interface is consistent with the radar image. In the cross-sectional view, the electromagnetic waves will vibrate when they pass through the upper surface of pipe area. Therefore, the vertical depth of pipe can be obtained according to the time and wave velocity of electromagnetic wave propagation in the pipe area.

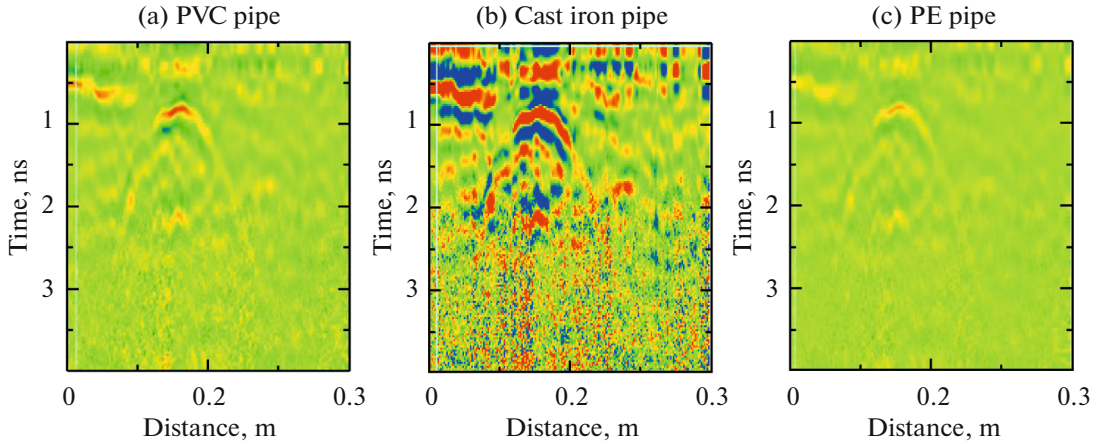

Fig. 10. Radar signal image of different material pipelines.

In Fig. 9a, the horizontal signals of the upper and lower surfaces for the electromagnetic wave passing through the pipeline are 0.5 and 2.1 ns respectively. The one-way travel time is half of the difference of coordinate values of 1.3 ns. The regional wave velocity is 7.48 cm/ns. The vertical depth of the pipe center is 9.72 cm, which is close to the actual vertical depth with 10 cm of the model. Similarly, the vertical depth of the pipe center is 15.71 cm in Fig. 9b, and the vertical depth of the pipe center is 24.68 cm in Fig. 9c.

According to the image, the vertical spacing of the pipelines with three depths on the radar profile is about 7.5 cm, which is the same as the actual separation distance. The detection results are relatively accurate at the relative spacing, but the absolute depth is different from the actual situation. The vertical resolution of the radar is not high enough, the original image has slightly changed the detection signal in the process of pre-processing such as direct-wave processing. Therefore, it should test more times to obtain the accurate depth in actual engineering.

3.4. Signal Analysis of Pipeline with Different Materials

The radar signal profile of different material pipes is shown in Fig. 10.

Comparing Figs. 10a, 10b and 10c, it can be found that the cast iron pipe has a more obvious hyperbolic in-phase axis than the PVC and PE pipes in the same diameter, the signal amplitude is large, the multiple waves are obvious, the image characteristics of PVC and PE pipes are more regular. The experimental results show that the radar image signal strength has little relationship with the dielectric constant value difference between the target detector and the medium. The dielectric constant is smaller, the signal amplitude is larger, and the signal characteristics are more obvious.

3.5. Analysis of Pipeline and Oil Pollution Radar Signal

The radar signal of sand (Fig. 11a) and the radar signal after the oil injection is injected for 20 min (Fig. 11b) are extracted separately. The oil leaks into the sand and spreads in the downward and outward diffusion. The dielectric properties of the sand in the model tank are changed, the dense diffraction signal can be generated in the radar signal profile. According to the data, it is known that the oil-like liquid medium has a relatively large relative dielectric constant, it is equivalent to a high-frequency filter in the electromagnetic wave transmission process, it is a low-frequency signal with a large wavelength in the lower part, it has fewer effective signals. The results show that ground penetrating radar can detect the change in the leakage of liquid media such as oil around the pipeline.

As shown in Figs. 11c–11e, after the oil is leaked, the radar profile shows the signal is changed in the oil diffusion direction and perpendicular to the oil diffusion direction on the longitudinal line, the top reflection wave is delayed, the bottom reflection is at the bottom of the oil contamination area. The wave has a superposition phenomenon, there is no obvious phase inflection point signal at the initial wave position of the oil bottom, it cannot determine the specific diffusion area of the oil according to the image.

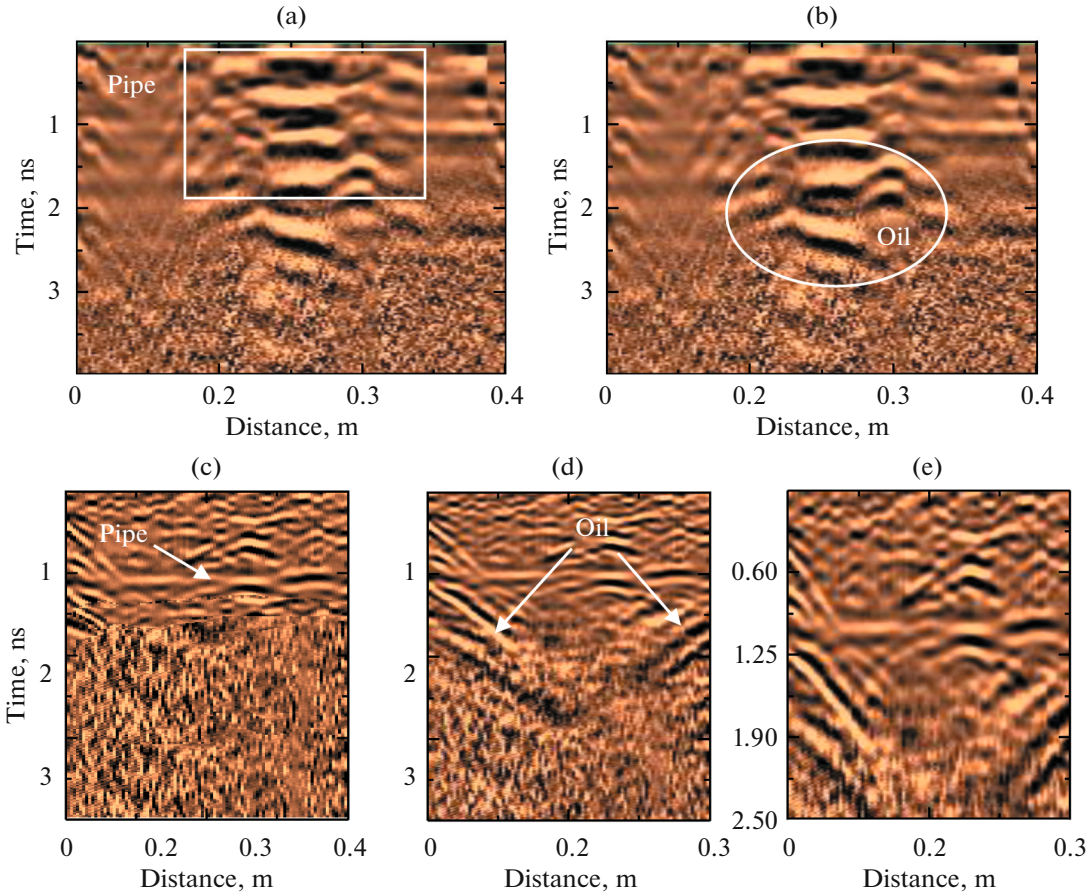

Fig. 11. Pipeline and leakage oil radar signal image. (a) Lateral signal when oil is injected; (b) lateral signal after 20 min of injection; (c) longitudinal signal when oil is injected; (d) longitudinal signal after 20 min of injection; (e) Partial enlargement of leakage oil (longitudinal).

4. CONCLUSIONS

There are few applications for the oil leakage detection in underground pipelines, based on the principle of ground penetrating radar detection technology, the indoor model test of underground pipelines and oil pipe leakage pipe-contaminated soil is carried out, the radar signals are qualitatively analyzed. The following conclusions are drawn:

(1) The band pass filtering, de-directing wave, background removal, etc. in the pre-processing step can effectively eliminate the interference signal and reduce the original image noise. The signal gain can significantly amplify the characteristic signal of detection target, which facilitates the identification of underground target. It also enhances the invalid signal to a certain extent, which is not conducive to the quantitative analysis of the detection target.

(2) The different sizes of the electromagnetic waves cause signal differences. The diameter of the pipe is larger, the radius of curvature of the hyperbola on the image is larger. The extension length at both ends id larger, the signal is clearer. At the same time, it is verified that the pipe diameter and vertical depth are proportional to the horizontal length and vertical length of strong reflection signal on the outer surface of signal region respectively.

(3) The RIS ground penetrating radar with 1600 MHz antenna for vertical depth resolution of underground pipeline is up to 5 cm, the quantitative detection error rate for pipeline buried depth is about 25%, the horizontal direction when pipeline spacing is greater than 8 cm can effectively display pipeline features, the horizontal direction resolution is not less than 8 cm.

(4) When the pipe is filled with oil, the liquid medium has the high dielectric constant, the hyperbolic interface of pipe is no longer obvious. The strong signal is accompanying the oil area, it shows a hyperbolic profile and no longer shows a clear in-phase axis. The characteristic signal of pipeline filled oil is the cres-

cent-shaped signal with the opening facing downward, the reflective area of pipeline is reduced, the absorption of electromagnetic waves is strong.

(5) The leakage oil changes the dielectric properties of sand in the model tank during the diffusion process to the soil layer, it can generate dense diffraction signals in the radar signal profile, which will filter the effective signal to some extent. As a result of the barrier, the process of migration and diffusion of oil can be successfully detected on the radar profile, but the existing results shows that it is difficult to quantitatively identify the oil area.

ACKNOWLEDGMENTS

Financial support comes from the National Natural Science Foundation of China (Grant no. 51508159), the Fundamental Research Funds for the Central Universities of Hohai University (no. 2019B12914), the Key Laboratory of Ministry of Education for Geomechanics and Embankment Engineering, Hohai University (no. GHXN201904) are gratefully appreciated.

REFERENCES

1. Shirokov, V.S., Soil and traffic loads on underground pipelines, *Soil Mech. Found. Eng.,* 2018, vol. 55, pp. 115–119.
2. Shin, S., Lee, G., Ahmed, U., Lee, Y., Na, J., and Han, C., Risk based underground pipeline safety management considering corrosion effect, *J. Hazard. Mater.,* 2018, vol. 342, pp. 279–289.
3. Shou, K.J. and Chen, B.C., Numerical analysis of the mechanical behaviors of pressurized underground pipelines rehabilitated by cured in place pipe method, *Tunnelling Underground Space Technol.,* 2018, vol. 71, pp. 544–554.
4. Li, W., Han, Y., Liu, Y., Zhu, C.R., Ren, Y.B., Wang, Y.J., and Chen, G., Real time location based rendering of urban underground pipelines, *Int. J. Geo-Inf.,* 2018, vol. 7, no. 1, p. 32.
5. Rashidov, T.R. and An, E.V., Geometrically nonlinear buckling stability analysis of axially loaded underground pipelines, *Soil Mech. Found. Eng.,* 2017, vol. 54, pp. 76–80.
6. Duru, C. and Ani, C., A statistical analysis on the leak detection performance of underground and overground pipelines with wireless sensor networks through the maximum likelihood ratio test, *Sadhana Acad. Proc. Eng. Sci.,* 2017, vol. 42, pp. 1889–1899.
7. Bors, A.M., Butoi, N., Caramitu, A.R., Marinescu, V., and Lingvay, I., The thermooxidation and resistance to moulds action of some polyethylene sorts used at anticorrosive insulation of the underground pipelines, *Mater. Plast.,* 2017, vol. 54, pp. 447–452.
8. Amaya Gomez, R., Ramirez Camacho, J.G., Pastor, E., Casal, J., and Munoz, F., Crater formation by the rupture of underground natural gas pipelines: A probabilistic based model, *J. Nat. Gas Sci. Eng.,* 2018, vol. 54, 224–239.
9. Gadala, I.M., Wahab, M.A., and Alfantazi, A., Electrochemical corrosion finite element analysis and burst pressure prediction of externally corroded underground gas transmission pipelines, *J. Pressure Vessel Technol. Trans. ASME,* 2018, vol. 1401, no. 1, p. 011701.
10. Gunduz, M. and Naser, A.F., Cost based value stream mapping as a sustainable construction tool for underground pipeline construction projects, *Sustainability,* 2017, vol. 9(12), p. 2184.
11. Kim, H.M. and Park, G.S., A new sensitive excitation technique in nondestructive inspection for underground pipelines by using differential coils,*IEEE Trans. Magn.,* 2017, vol. 53, no. 11, pp. 1–4, article ID 6202604.
12. Dzhala, RM., Verbenets, B.Y., Mel'nyk, M.I., Mytsyk, A.B., Savula, R.S., and Semenyuk, O.M., New methods for the corrosion monitoring of underground pipelines according to the measurements of currents and potentials, *Mater. Sci.,* 2017, vol. 52, pp. 732–741.
13. Israilov, M.S., Mardonov, B., and Rashidov, T.R., Seismodynamics of an underground pipeline in nonideal contact with soil: Effect of sliding on dynamic stresses, *J. Appl. Mech. Tech. Phys.,* 2016, vol. 57, pp. 1126–1132.
14. Dimov, LA. and Dimov, I.L., New way of determining soil resistance to underground pipeline deformation, *Soil Mech. Found. Eng.,* 2016, vol. 53, pp. 312–316
15. Sahraoui, Y. and Chateauneuf, A., The effects of spatial variability of the aggressiveness of soil on system reliability of corroding underground pipelines, *Int. J. Pressure Vessels Piping,* 2016, vol. 146, pp. 188–197.
16. Ha, H.M. and Alfantazi, A., On the role of water, temperature, and glass transition in the corrosion protection behavior of epoxy coatings for underground pipelines, *J. Coatings Technol. Res.,* 2015, vol. 12, pp. 1095–1110.
17. Khan, L.R. and Tee, K.F., Quantification and comparison of carbon emissions for flexible underground pipelines, *Can. J. Civ. Eng.,* 2015, vol. 42, pp. 728–736.
18. Matvienko, A.F., Korzunin, G.S., Loskutov, V.E., and Babkin, S.A., The quality control of underground gas pipelines via the electromagnetic and acoustic method, *Russ. J. Nondestr. Test.,* 2015, vol. 51, pp. 546–553.

19. Guo, Z.Y., Liu, D.J., Pan, Q., Zhang, Y.Y., Li, Y., and Wang, Z., Vertical magnetic field and its analytic signal applicability in oil field underground pipeline detection, *J. Geophys. Eng.,* 2015, vol. 12, pp. 340–350.
20. Klesk, P., Kapruziak, M., and Olech, B., Statistical moments calculated via integral images in application to landmine detection, *Pattern Anal. Appl.,* 2018, vol. 21, pp. 671–684.
21. Sun, H., Pashoutani, S., and Zhu, J., Nondestructive evaluation of concrete bridge decks with automated acoustic scanning system and ground penetrating radar, *Sensors,* 2018, vol. 18, p. 1955.
22. Dinh, K., Gucunski, N., and Duong, T.H., An algorithm for automatic localization and detection of rebars from GPR data of concrete bridge decks, *Autom. Constr.,* 2018, vol. 89, pp. 292–298.
23. Dinh, K., Gucunski, N., and Kim, J., Method for attenuation assessment of GPR data from concrete bridge decks, *NDT & E Int.,* 2017, vol. 92, pp. 50–58.
24. Dinh, K., Gucunski, N., and Kim, J., Understanding depth–amplitude effects in assessment of GPR data from concrete bridge decks, *NDT & E Int.,* 2016, vol. 83, pp. 45–58.
25. Gucunski, N., Pailes, B., and Kim, J., Capture and quantification of deterioration progression in concrete bridge decks through periodical NDE surveys, *J. Infrastruct. Syst.,* 2017, vol. 23, no. 1.
26. Romero, F.A., Barnes, C.L., and Azari, H., Validation of benefits of automated depth correction method: improving accuracy of ground–penetrating radar deck deterioration maps, *Transp. Res. Board.,* 2015, vol. 1.
27. Ukaegbu, I.K. and Gamage, K.A.A., Ground penetrating radar as a contextual sensor for multi-sensor radiological characterization, *Sensors,* 2017, vol. 17, no. 4, p. 790.